JOURNAL OF VIROLOGY, May 2002, p. 4688–4698 Vol. 76, No. 10
0022-538X/02/$04.00+0 DOI: 10.1128/JVI.76.10.4688–4698.2002

Kaposi's Sarcoma-Associated Herpesvirus OX2 Glycoprotein Activates Myeloid-Lineage Cells To Induce Inflammatory Cytokine Production

Young-Hwa Chung, Robert E. Means, Joong-Kook Choi, Bok-Soo Lee, and Jae U. Jung*

Department of Microbiology and Molecular Genetics and Tumor Virology Division, New England Regional Primate Research Center, Harvard Medical School, Southborough, Massachusetts 01772

Received 8 January 2002/Accepted 20 February 2002

Kaposi's sarcoma is an inflammatory cytokine-mediated angioproliferative disease which is triggered by infection by Kaposi's sarcoma-associated herpesvirus (KSHV). KSHV contains an open reading frame, K14, that has significant homology with cellular OX2, designated viral OX2 (vOX2). In this report, we demonstrate that vOX2 encodes a glycosylated cell surface protein with an apparent molecular mass of 55 kDa. Purified glycosylated vOX2 protein dramatically stimulated primary monocytes, macrophages, and dendritic cells to produce the inflammatory cytokines interleukin 1β (IL-1β), IL-6, monocyte chemoattractant protein 1, and TNF-α. Furthermore, expression of vOX2 on B lymphocytes stimulated monocytes to produce inflammatory cytokines in mixed culture. These results demonstrate that like its cellular counterpart, vOX2 targets myeloid-lineage cells, but unlike cellular OX2, which delivers a restrictive signal, KSHV vOX2 provides an activating signal, resulting in the production of inflammatory cytokines. Thus, this is a novel viral strategy where KSHV has acquired the cellular OX2 gene to induce inflammatory cytokine production, which potentially promotes the cytokine-mediated angiogenic proliferation of KSHV-infected cells.

Kaposi's sarcoma (KS) is a multifocal angiogenic tumor consisting of characteristic spindle cells and infiltrating leukocytes (43). KS occurs in several epidemiologically distinct forms and is the most common AIDS-associated tumor (33, 40). Unlike most cancers, KS does not appear to be due to clonal expansion of a transformed cell. Instead, it appears to be a hyperplastic disorder caused, in part, by local production of inflammatory cytokines such as interleukin 1 (IL-1), IL-6, gamma interferon (IFN-γ), and tumor necrosis factor alpha (TNF-α) and growth factors such as basic fibroblast growth factor and vascular endothelial growth factor (11–14). This is supported by the fact that infiltration of inflammatory cells in KS lesions, including $CD8^+$ T cells, monocytes, macrophages, and dendritic cells, precedes transformation of the spindle-shaped endothelial cells (3, 26, 39). Infiltrating cells systematically produce inflammatory cytokines that are likely responsible for activation of vessels and endothelial cells, increase of adhesiveness with extravasation, and recruitment of lymphocytes and monocytes (10, 12).

Based on strong epidemiological and histopathological association, KS-associated herpesvirus (KSHV), or human herpesvirus 8, is thought to be an etiologic agent of KS. KSHV has been consistently identified in KS tumors from human immunodeficiency virus-positive and -negative patients (6, 7, 30). KSHV has also been identified in primary effusion lymphoma (PEL) and an immunoblast variant of Castleman's disease, which are of B-cell origin (6, 7, 41). The genomic sequence classifies KSHV as a gamma-2 herpesvirus that is closely related to herpesvirus saimiri (32, 42) and rhesus monkey rhadinovirus (RRV) (8, 45).

How KSHV induces KS is not known; however, the viral genomic sequence has provided important clues that together strengthen the prevailing theory of cytokine- and growth factor-mediated pathogenesis. In particular, DNA sequence analysis of the KSHV genome predicts that the K14 open reading frame exhibits a significant level of homology with cellular OX2, now designated viral OX2 (vOX2). Cellular OX2 belongs to a group of leukocyte glycoproteins with a broad expression profile. Both stimulatory and tolerogenic roles for OX2 in antigen presentation have been proposed (2, 18). Specifically, OX2 antigen has been shown to provide a costimulatory signal for activated T cells, leading to an increase of IL-4 and transforming growth factor alpha production but not IL-2 production (2). In contrast, unlike conventional costimulatory molecules, such as CD40, CD80, and CD86, OX2 has been shown to deliver negative signals to T cells and macrophages upon antigen recognition, resulting in decreased graft rejection in animals (17, 19). Furthermore, the disruption of the OX2 gene in mice leads to expansion of the macrophage and granulocyte populations in mesenteric lymph nodes, supporting the role of OX2 in attenuation of signaling in monocyte lineage cells (20). Recently, an OX2 receptor (OX2R) has been identified as a novel protein having a restricted expression in cells of the myeloid lineage (48). OX2-OX2R interaction delivers a restrictive signal to macrophages and thus limits macrophage activation. Subsequently, blocking of this interaction with anti-OX2R antibody exacerbates tissue damage in inflammatory sites (48).

In this report, we demonstrate that vOX2 encodes a glycosylated protein with an apparent molecular mass of 55 kDa, is expressed on the surface of KSHV-infected cells during viral lytic replication, and targets myeloid-lineage cells. Unlike cellular OX2, which delivers a restrictive signal to myeloid-lin-

* Corresponding author. Mailing address: Tumor Virology Division, New England Regional Primate Research Center, Harvard Medical School, P.O. Box 9102, 1 Pine Hill Dr., Southborough, MA 01772-9102. Phone: (508) 624-8083. Fax: (508) 786-1416. E-mail: jae_jung@hms.harvard.edu.

eage cells, KSHV vOX2 provides an activating signal to myeloid-lineage cells and thus, induces their inflammatory cytokine production. Thus, KSHV vOX2 targets and activates cells of myeloid lineage to produce inflammatory cytokines, which potentially recruit lymphocytes to the site of the infection, subsequently disseminates virus throughout infected hosts, and further promotes the cytokine-mediated proliferation of KSHV-infected cells.

MATERIALS AND METHODS

Cell culture and transfection. 293T cells were grown in Dulbecco's modified Eagle's medium supplemented with 10% fetal calf serum. U937 myeloid leukemia cells and BJAB, BCBL-1, and JSC-1 cells were grown in RPMI 1640 supplemented with 10% fetal calf serum. BCBL-1 and JSC-1 cells were induced with phorbol-12-tetradecanoate-13-acetate (TPA, 20 ng/ml). Fugene 6 (Roche, Indianapolis, Ind.) or calcium phosphate (Clontech, Palo Alto, Calif.) was used for transient expression of vOX2 in 293T cells, and electroporation at 260 V and 975 μF was used for transient expression of vOX2 in BJAB cells. A stable BJAB cell line expressing vOX2 was selected and maintained by the presence of G418 (1 mg/ml).

Cloning of KSHV vOX2 DNA from BCBL-1 cells. A DNA fragment corresponding to the KSHV vOX2 coding sequence was amplified from BCBL-1 genomic DNA by PCR. Specifically, the second methionine of the predicted vOX2 (42) was used as an initiation codon. PCR-amplified DNA was cloned into the pEF-His vector (Invitrogen, San Diego, Calif.). To construct the amino-terminal hemagglutinin (HA)-tagged vOX2, KSHV vOX2 (amino acids 100 to 348) without the putative signal peptide sequence was amplified by PCR and subcloned into the pDisplay-HA vector (Invitrogen). KSHV vOX2 DNA was completely sequenced to verify 100% agreement with the original sequence with a ABI PRISM 377 automatic DNA sequencer.

Recombinant vOX2-GST and OX2-GST protein and antibody production. The extracellular portion (amino acids 1 to 303 or 78 to 303) of the predicted vOX2 protein (42) and the extracellular portion (amino acids 1 to 234) of the human OX2 gene were fused in frame into glutathione *S*-transferase (GST) gene. vOX2 and OX2 DNA fragments were amplified by PCR with primers containing *Kpn*I and *Bam*HI recognition sequences at the ends and subcloned into *Kpn*I and *Bam*HI cloning sites of the pDEF3-GST vector (15). The absence of unwanted mutations was confirmed by DNA sequencing. The plasmid prepared by CsCl ultracentrifugation was transfected into 293T cells by the calcium phosphate method (Clontech) according to the manufacturer's instructions. The supernatant of 293 T cells was harvested 5 days posttransfection, and secreted glycosylated vOX2-GST fusion and OX2-GST fusion proteins were purified with a glutathione-Sepharose column (Clontech) and eluted with 40 mM glutathione. Control GST protein was purified from pDEF3-GST-transfected 293 T cells with a glutathione-Sepharose column. Purified proteins were dialyzed against phosphate-buffered saline (PBS) overnight. To generate mouse antibody, the purified vOX2-GST protein was administered to BALB/c mice (6 to 10 weeks old; Charles River, Southbridge, Mass.) intraperitoneally three times at 1-week intervals.

Immunoblotting and antibodies. Cells were harvested and lysed with lysis buffer (0.15 M NaCl, 1% Nonidet P-40, 50 mM Tris; pH 7.5) containing 0.1 mM Na_2VO_3, 1 mM NaF, and protease inhibitors (leupeptin, aprotinin, phenylmethylsulfonyl fluoride, and bestatin). For immunoblots, polypeptides from whole-cell lysates were resolved by sodium dodecyl sulfate-polyacrylamide gel electrophoresis (SDS-PAGE) and transferred to nitrocellulose membrane filters. Immunoblot detection was performed with a 1:2,000 dilution of vOX2 antibody, anti-AU1 antibody (Covance, Berkeley, Calif.), anti-GST antibody (Santa Cruz Biotech, Santa Cruz, Calif.), or a 1:1,000 dilution of anti-His antibody (Santa Cruz Biotech). The protein was visualized with a chemical luminescent detection reagent (Pierce, Rockford, Ill.) and detected with a Fuji Phospho Imager.

Immunofluorescence tests. Cells were fixed with 4% paraformaldehyde for 15 min, permeabilized with cold acetone for 15 min, blocked with 10% goat serum in PBS for 30 min, and reacted with 1:100-diluted primary antibody in PBS for 30 min at room temperature. Confocal immunofluorescence was performed as previously described (21).

FACS analysis. Cells (5×10^5) were washed with RPMI medium containing 10% fetal calf serum and incubated with mouse polyclonal vOX2 antibody, preimmunized mouse sera, or anti-HA antibody (Santa Cruz) followed by fluorescein isothiocyanate (FITC)-conjugated anti-mouse antibodies (Pharmingen) for 30 min at 4°C. After washing, each sample was fixed with 1% paraformaldehyde solution, and fluorescence-activated cell sorting FACS analysis was performed with a FACScan (Becton Dickinson, Mountain View, Calif.).

Measurement of cytokine production by ELISA. Peripheral blood mononuclear cells (PBMCs) from healthy donors were prepared by Ficoll density gradient purification as previously described (9). T cells, B cells, and monocytes /macrophages were sorted by flow cytometry (FACS Vantage; Becton Dickinson) using anti-CD3, anti-CD19, and anti-CD14 antibodies. Human dendritic cells were purchased from Clonetics (San Diego, Calif.). These cells were isolated from PBMCs by leukapheresis and density gradient centrifugation to pure population, cultured in the commercial medium provided by Clonetics, and tested for CD11C and CD86 surface expression. After 48 h of resting, 1×10^5 to 2×10^5 purified cells were seeded into flat-bottom 96-well plates in the absence or presence of IFN-γ (100 U/ml; Gibco-BRL). Thereafter, vOX2-GST (1 μg/ml), OX2-GST (1 μg/ml), GST (1 μg/ml), or RPMI medium as a mock treatment was added to each well. After 48 h of incubation, supernatants were harvested and used for the measurement of IL-1β, TNF-α, IL-6, and monocyte chemoattractant protein 1 (MCP-1) production using specific Pharmingen enzyme-linked immunosorbent assay (ELISA) kits. U937 monocytes (1×10^5) were mixed with BJAB cells or BJAB cells expressing vOX2 (BJAB-vOX2 cells) (4×10^5) in the 24-well plate in the absence or presence of IFN-γ (200 U/ml). The supernatants were harvested after 48 h of incubation and measured for the production of IL-1β, IL-12, and TNF-α by ELISA.

RESULTS

Identification of vOX2. Initial DNA sequence analysis of the KSHV genome predicts that the putative vOX2 protein contains 348 amino acids, which is considerably longer than cellular OX2 (278 amino acids) and RRV R14 (253 amino acids), which is a homologue of KSHV vOX2 (1, 45). In addition, unlike cellular OX2 and RRV R14, the predicted KSHV vOX2 protein does not contain the typical signal peptide sequence in its amino-terminal region. However, careful inspection reveals that the second methionine (amino acid residue 78) of vOX2 appears to be more likely to function as the initiation codon. This would give a protein of 271 amino acids with a typical signal peptide sequence and with a size similar to those of cellular OX2 and RRV R14. Regardless of which initiation codon is utilized, vOX2 contains five potential N-glycosylation sites in its extracellular domain.

To identify a functional signal peptide sequence in the KSHV vOX2 protein, we used the pDEF-GST-AU1 expression plasmid, which contains the elongation factor promoter and multicloning sites linked to a C-terminal AU1 epitope-tagged GST gene. Amino acids 1 to 303 or 78 to 303 of vOX2, which both contained the putative extracellular region without transmembrane and cytoplasmic regions, were fused in frame into GST-AU1 to create the $vOX2_L$-GST and $vOX2_S$-GST chimeras, respectively. At 72 h after transfection with the vOX2-GST expression vectors, supernatants from 293T cells were harvested. Since a functional signal peptide would be capable of directing secretion of the vOX2-GST protein, supernatants of the transfected cells were mixed with glutathione beads and subjected to immunoblot assay with anti-GST antibody or anti-AU1 antibody. This showed that $vOX2_L$-GST and $vOX2_S$-GST exhibited the same 65-kDa molecular mass in SDS-PAGE (Fig. 1A and data not shown). This indicates that the second methionine of vOX2 at amino acid 78 is used as an initiation codon. Thus, the revised vOX2 coding sequence containing the second methionine as an initiation codon was used throughout the study.

To purify a large quantity of vOX2-GST protein, 20 liters of supernatants from 293T cells transfected with the pDEF-vOX2-GST expression vector was subjected to glutathione af-

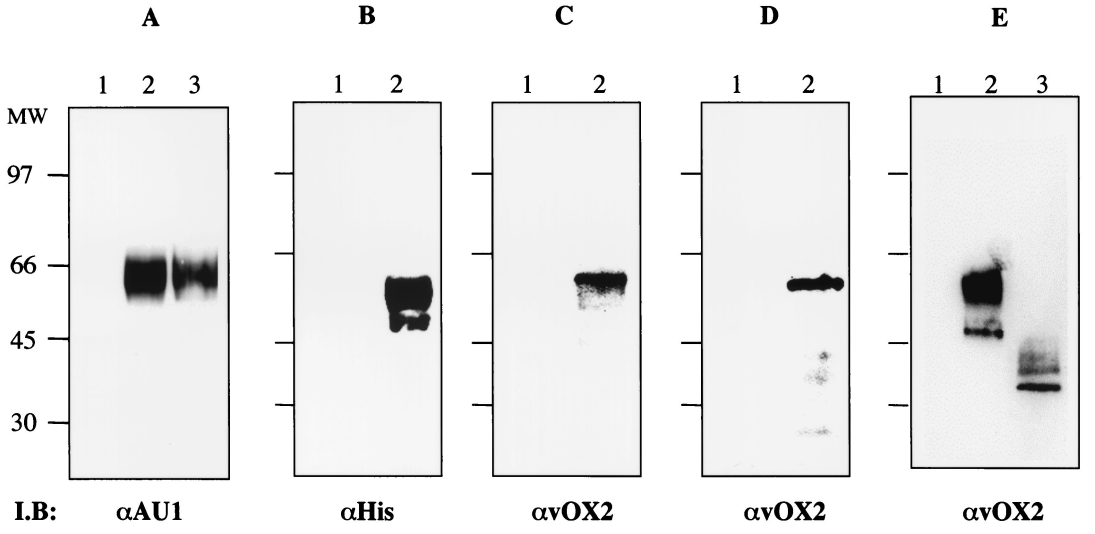

FIG. 1. Identification of vOX2 protein and its glycosylation. (A) Comparison of $vOX2_S$-GST protein and $vOX2_L$-GST protein. 293T cells were transfected with expression vector pDEF3-$vOX2_S$-GST-AU1 or pDEF3-$vOX2_L$-GST-AU1. At 48 h posttransfection, supernatants were harvested and run on a glutathione-Sepharose resin column. Partially purified proteins were subjected to immunoblotting (I.B) with an anti-AU1 antibody. Lane 1, untransfected cell supernatant; lane 2, $vOX2_S$-GST-AU1; lane 3, $vOX2_L$-GST-AU1. (B and C) Identification of vOX2 protein in 293T cells. At 48 h posttransfection, 293T cells were lysed, and whole-cell lysates were separated by SDS-PAGE, transferred to nitrocellulose membranes, and reacted with anti-His (B) or anti-vOX2 (C) antibody. Lane 1, 293T cells transfected with pEF vector; lane 2, 293T cells transfected with pEF-vOX2 vector. (D) Identification of vOX2 protein in KSHV-infected PEL cells. Lysates of BJAB cells (lane 1) and JSC1 cells (lane 2) were used for immunoblot assay with an anti-vOX2 antibody. (E) N glycosylation of vOX2 protein. AT 48 h after transfection with pEF-vOX2, 293T cells were lysed, and whole-cell lysates were treated with *N*-glycosidase for 12 h and then subjected to immunoblot assay with an anti-vOX2 antibody. Lane 1, whole-cell lysates of 293T cells transfected with pEF; lane 2, whole-cell lysates of 293T cells transfected with pEF-vOX2; lane 3, *N*-glycosidase-treated whole-cell lysates of 293T cells transfected with pEF-vOX2. The data were reproduced in at least two independent experiments.

finity chromatography. vOX2-GST protein was eluted by 40 mM glutathione and dialyzed against PBS overnight. Protein staining showed that vOX2-GST fusion protein secreted to the supernatant was purified to virtual homogeneity in one step by glutathione affinity chromatography (data not shown). Purified vOX2-GST specifically reacted with anti-AU1 and anti-GST antibodies (data not shown). Using purified vOX2-GST, a mouse polyclonal antibody was generated. Two days after transfection with an expression vector containing full-length vOX2 that contained a His epitope tag at its carboxyl terminus, 293T cells were lysed and whole-cell lysates were used for immunoblot assay with an anti-vOX2 mouse polyclonal antibody and an anti-His rabbit polyclonal antibody. Both the anti-vOX2 antibody and anti-His antibody specifically reacted with a 55-kDa protein as the major species and a 50-kDa protein as the minor species (Fig. 1B and C, lanes 2). Furthermore, the anti-vOX2 antibody specifically reacted with a 55-kDa protein from KSHV-infected JSC-1 cells, the same molecular mass as vOX2 protein from 293T cells (Fig. 1D, lane 2). In contrast, vOX2 protein was not detected in control 293T cells without vOX2 expression (Fig. 1B and C, lanes 1) or in control KSHV-negative BJAB cells (Fig. 1D, lane 1). These results further support the idea that the second methionine is used as an initiation codon for vOX2 protein.

The potential N-linked glycosylation in the extracellular region of vOX2 likely contributed to the slow migration of vOX2 protein in SDS-PAGE. To test this, lysates of 293T cells transfected with pEF-vOX2 were treated with *N*-glycosidase, which cleaves N-linked oligosaccharides. Upon *N*-glycosidase treatment, the 55- and 50-kDa proteins disappeared and the 40- and 35-kDa proteins became the major bands (Fig. 1E). These results indicate that vOX2 is modified by N glycosylation and the 55-kDa protein is likely a mature form of vOX2.

Lytic expression of KSHV vOX2 surface protein. The localization of vOX2 was determined by indirect immunofluorescence tests. 293T cells transfected with the vOX2 expression vector were permeabilized with acetone and stained with the anti-vOX2 antibody. The staining pattern suggested that vOX2 was principally associated with the plasma membrane (Fig. 2A).

To further examine vOX2 expression, vOX2 gene was tagged in its extracellular domain with an HA epitope downstream of the predicted signal peptide sequence cleavage site to generate HA-vOX2. At 48 h after transfection with pDisplay-HA-vOX2, BJAB cells were fixed and stained with anti-OX2 and anti-HA antibodies. Flow cytometry analysis showed positive surface staining of transfected BJAB cells with anti-vOX2 and anti-HA antibodies (Fig. 2B). Transfected BJAB cells were further selected with 1 mg of G418 per ml for the next 5 weeks. Flow cytometry analysis also showed that vOX2 was expressed on the surfaces of G418-resistant BJAB cells (data not shown). These results demonstrate that vOX2 is expressed on the surfaces of transfected cells and that the amino-terminal region of vOX2 is exposed to the extracellular milieu, indicating a type I transmembrane structure of vOX2.

KSHV/Epstein-Barr virus (EBV)-infected JSC-1 cells maintain a tightly regulated latent replication of KSHV; however, TPA stimulation efficiently induces lytic replication of KSHV (5). To detect surface expression of vOX2, JSC-1 cells were stimulated with TPA for 0, 24, 48, and 72 h, followed by flow

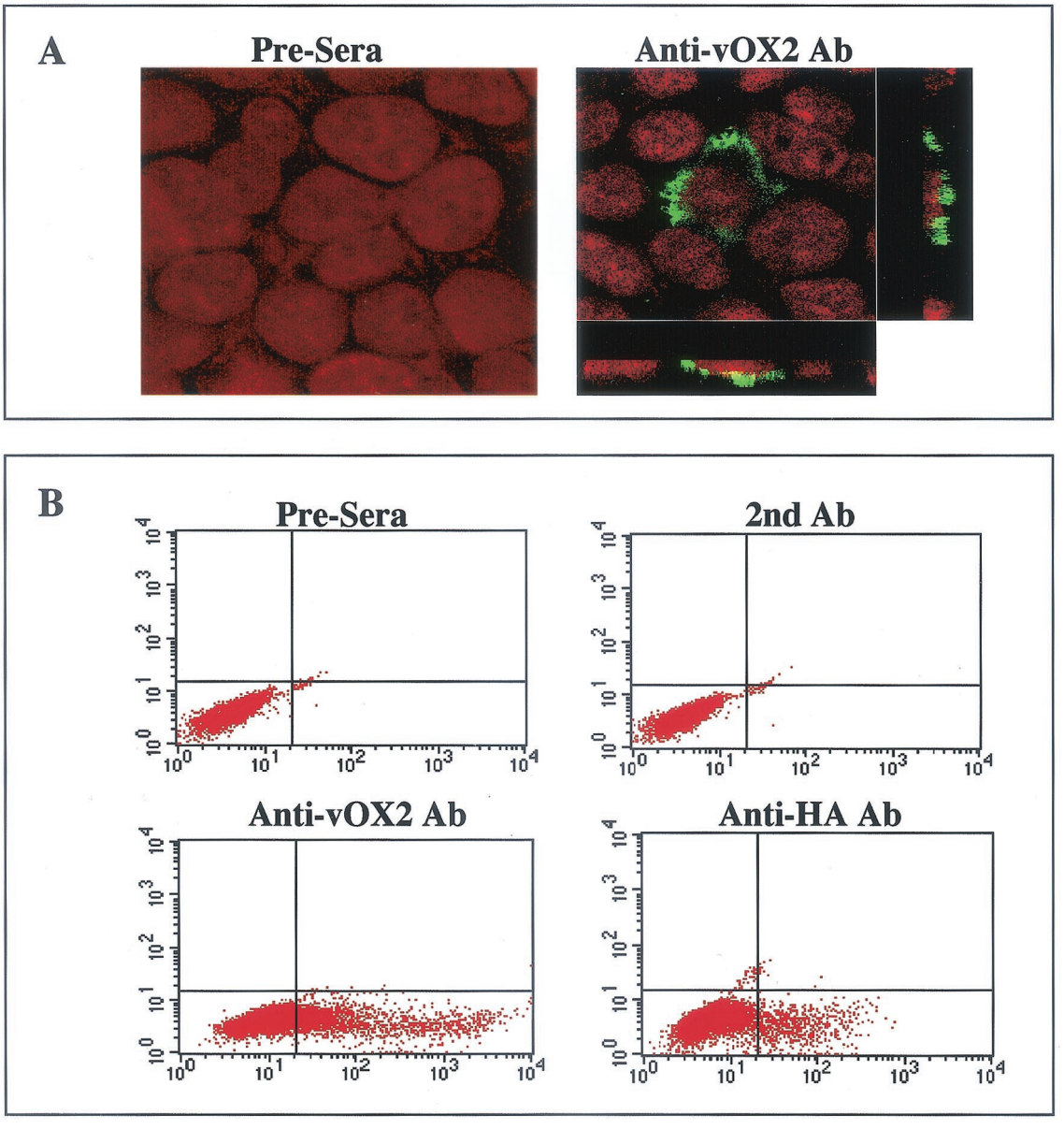

FIG. 2. Surface expression of vOX2. (A) Plasma membrane localization of vOX2. At 48 h posttransfection, 293T cells transfected with pEF-vOX2 were fixed with paraformaldehyde, permeabilized with acetone, and reacted with preimmune sera (Pre-sera) or an anti-vOX2 antibody, followed by FITC-conjugated anti-mouse secondary antibody (green). Cells were additionally stained with To-pro solution (red; Molecular Probes, Eugene, Oreg.) for a minute to show the nucleus. Immunofluorescence was examined with a Leica confocal immunofluorescence microscope, and a single representative optical section is presented. To further determine its specific location, stained cells were cross-sectioned and viewed under the Leica confocal immunofluorescence microscope (side boxes). (B) Surface expression of vOX2 in transient expression. To examine the surface expression of vOX2, BJAB cells were electroporated with the pDisplay-HA-vOX2 plasmid. Surface expression of vOX2 on transfected BJAB cells was assessed 48 h posttransfection by staining with preimmune mouse sera, anti-vOX2 mouse polyclonal antibody, or anti-HA mouse monoclonal antibody, followed by FITC-conjugated anti-mouse antibody (secondary antibody). The right lower quadrants show vOX2 surface expression. The data were reproduced in at least two independent experiments.

cytometry analysis with an anti-vOX2 antibody as described above. While a significant level of vOX2 expression was detected on unstimulated JSC-1 cells by flow cytometry, the level of vOX2 expression gradually increased in JSC-1 cells during TPA stimulation (Fig. 3A). To further test expression of vOX2, KSHV/EBV-positive JSC-1 cells and KSHV/EBV-negative BJAB cells were used for immunoblot assays. After 0, 12, 24, and 72 h of TPA stimulation, JSC-1 cells were lysed and whole-cell lysates were reacted with an anti-vOX2 antibody. Additional antibodies to KSHV proteins were included in this assay: these were latently associated nuclear antigen (LANA) for detection of latent infection, MIR1 (K3) for immediate early lytic replication, viral IFN regulatory factor (vIRF) for early lytic replication, and K8.1 glycoprotein for late replication. Finally, cellular actin was included as a control for protein loading. It showed that the 55-kDa vOX2 protein was weakly

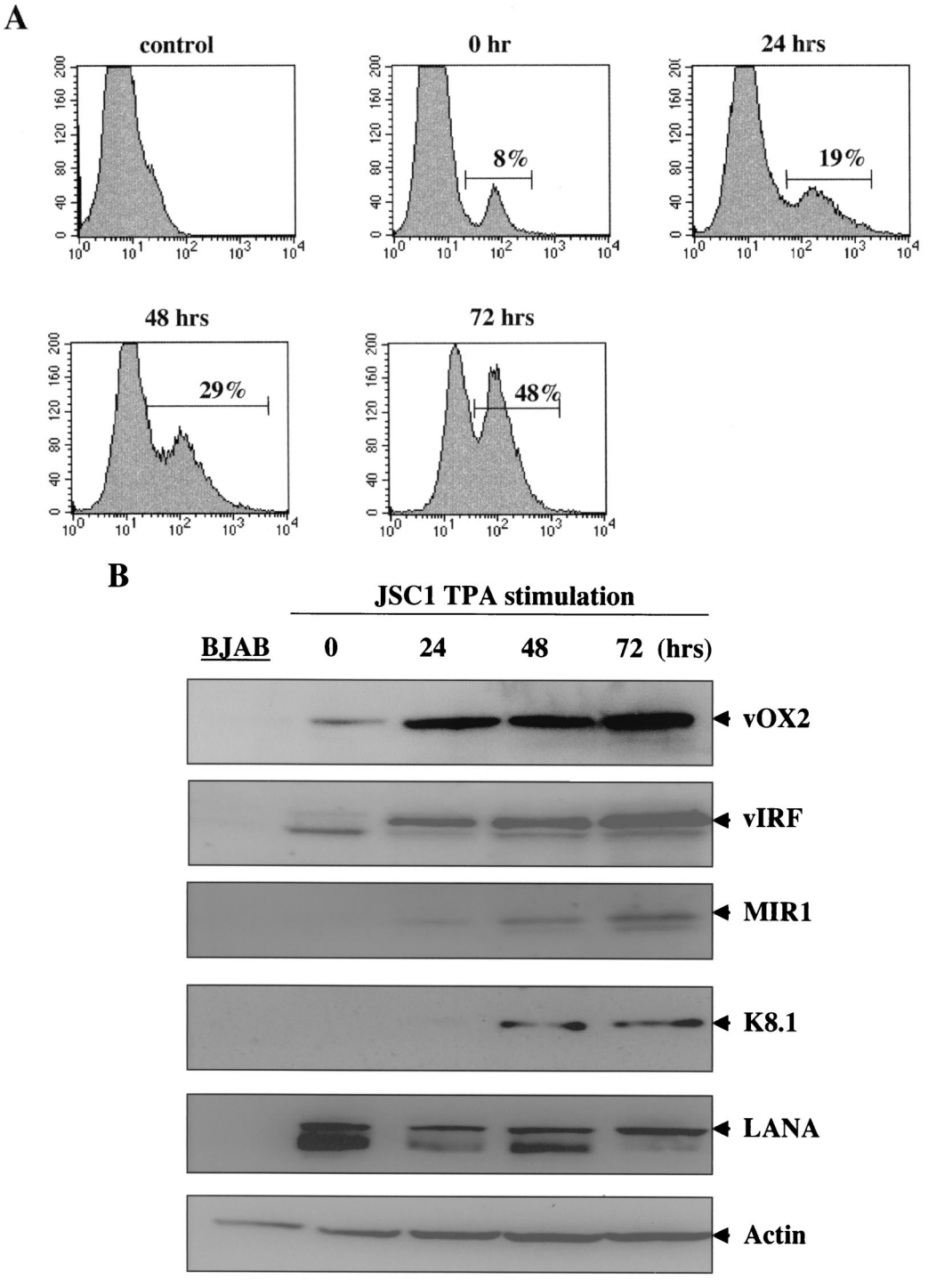

FIG. 3. Lytic expression of vOX2. (A) Flow cytometry analysis of vOX2 surface expression. Unstimulated JSC-1 or TPA-stimulated JSC-1 cells were reacted with an anti-vOX2 antibody, followed by FITC-conjugated anti-mouse immunoglobulin G. As a negative control, unstimulated JSC-1 cells were stained with FITC conjugated anti-mouse immunoglobulin G. Percentages are vOX2-positive cells. (B) vOX2 expression during to KSHV lytic replication. Unstimulated JSC-1, TPA-stimulated JSC-1 cells, or BJAB cell lysates were separated by SDS-PAGE, transferred to nitrocellulose membrane, and reacted with mouse anti-vOX2 antibody, rabbit anti-vIRF antibody, rabbit anti-K8.1 antibody, rabbit anti-MIR1 antibody, and rabbit anti-LANA antibody. As an internal control, donkey antiactin antibody was used.

detected in unstimulated JSC-1 cells and in increased amounts after TPA stimulation, whereas it was not detected in control BJAB cells (Fig. 3B). As shown previously (23, 28, 35, 38, 44), LANA, MIR1, vIRF, and K8.1 were primarily detected as KSHV latent, immediate early, early, and late lytic proteins, respectively (Fig. 3B). In addition, an equivalent amount of cellular actin was detected in all lanes (Fig. 3B). These results demonstrate that vOX2 is located principally on the plasma

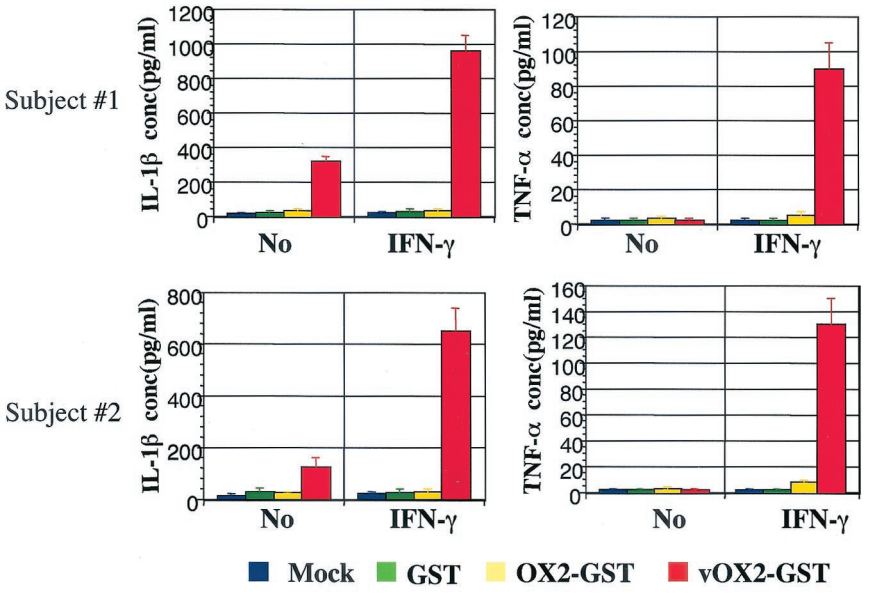

FIG. 4. Induction of inflammatory cytokine production in human PBMCs by vOX2-GST protein. PBMCs of healthy subjects were isolated and incubated with 1 μg of GST, vOX2-GST, or OX2-GST per ml or medium as a mock treatment in the absence or presence of IFN-γ (100 U/ml). The supernatants were harvested after 2 days of incubation and measured for the production of IL-1β and TNF-α cytokines by ELISA. Data are averages from triplicate measurements, and error bars indicate standard deviations.

membrane, that the amino terminus of vOX2 is exposed to the extracellular milieu, and that it is expressed on a minor population of unstimulated KSHV-infected PEL cells with enhanced expression, which was further enhanced during lytic replication of KSHV.

Induction of IL-1β and TNF-α production by vOX2-GST protein. Cellular OX2 belongs to a group of leukocyte immunoglobulin gene superfamily glycoproteins with a broad expression profile and delivers a restrictive signal to myeloid-lineage cells (20, 48). To study role of vOX2 in host lymphocyte signal transduction, purified GST (1 μg/ml), glycosylated vOX2-GST protein (1 μg/ml), or glycosylated OX2-GST protein (1 μg/ml) was added to PBMCs from two healthy participants. After 2 days of incubation with purified proteins, supernatants were harvested and subjected to ELISA. IL-1β production was detected from unstimulated PBMCs after vOX2-GST treatment, and it was further increased in IFN-γ-stimulated PBMCs after vOX2-GST treatment (Fig. 4). vOX2-GST fusion protein also showed a similar effect on TNF-α production in IFN-γ-stimulated PBMCs (Fig. 4). In contrast, GST and OX2-GST proteins did not induce IL-1β and TNF-α production under the same conditions (Fig. 4). To demonstrate the specificity of the vOX2 effect on inflammatory cytokine production, vOX2-GST protein was depleted by running it on a glutathione affinity column. Depletion of vOX2-GST protein drastically reduced its activity in IL-1β and TNF-α production, indicating a specific effect of vOX2 on inflammatory cytokine production (data not shown). These results demonstrate that an unlike cellular OX2, vOX2 stimulates PBMCs to induce inflammatory cytokine production.

Myeloid-lineage cells are targets for vOX2. Recently, an OX2R has been identified as a novel protein whose expression is restricted to cells of the myeloid lineage. The interaction between OX2 and OX2R has been shown to deliver a restrictive signal to macrophages and thus limits macrophage activation (20, 48). To identify specific lymphocytes targeted by vOX2, PBMCs were sorted into CD3-positive T cells, CD19-positive B cells, CD14-positive monocytes/macrophages, and CD11C/CD86-positive dendritic cells by FACS, and each group was analyzed for inflammatory cytokine production upon vOX-GST treatment. Each population of cells obtained by FACS was >95% pure. After sorting, they were rested for 2 days, followed by stimulation with or without IFN-γ overnight. After additional treatment with GST or vOX2-GST protein or mock treatment for 2 days, supernatants were harvested and subjected to ELISA to measure IL-1β and TNF-α production. IFN-γ-stimulated monocytes/macrophages and dendritic cells produced extensive amounts of IL-1β and TNF-α upon vOX2-GST treatment, whereas T and B cells did not under the same conditions (Fig. 5). As seen in Fig. 4, a small amount of IL-1β and TNF-α was also produced from unstimulated monocytes/macrophages and dendritic cells upon vOX2-GST treatment (Fig. 5). Furthermore, a strong aggregation was detected in unstimulated dendritic cells after treatment with vOX2-GST protein but not with GST protein (Fig. 6). In addition, an effect of vOX2-GST protein on aggregation was further enhanced by costimulation with IFN-γ (Fig. 6).

vOX2-GST- and GST-treated cells were further tested for the production of additional inflammatory cytokines and chemokines, including IL-6. vOX2-GST treatment weakly induced IL-6 production from unstimulated monocytes/macrophages and dendritic cells (Fig. 7). Since IFN-γ stimulation induced extensive amounts of IL-6 from myeloid-lineage cells, treatment with vOX2-GST did not show a significant effect on IL-6 production by these cells (Fig. 7 and data not shown). In addition, vOX2-GST treatment marginally induced MCP-1

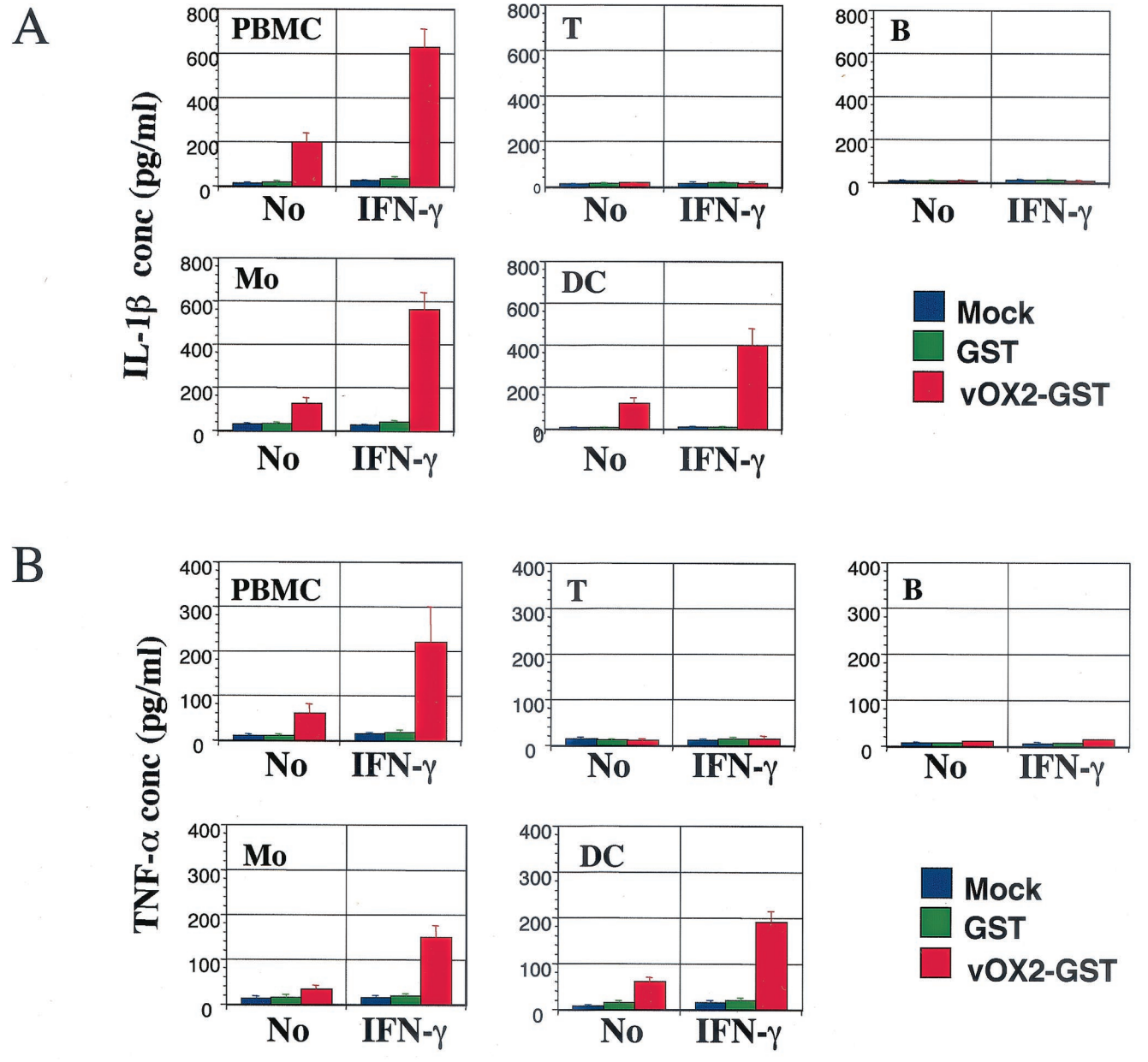

FIG. 5. vOX2-GST protein targets myeloid-lineage cells to induce inflammatory cytokine production. T cells (T), B cells (B), monocytes/macrophages (Mo), and dendritic cells (DC) were sorted by flow cytometry. Each lymphocyte (10^5) was incubated with 1 μg of GST or vOX2-GST per ml or medium as a mock treatment in the absence or presence of IFN-γ (100 U/ml). At 48 h postincubation, the supernatants were harvested and measured for production of IL-1β (A) and TNF-α (β) by ELISA. Data are averages from triplicate measurements, and error bars indicate standard deviations.

production from unstimulated monocytes/macrophages and dendritic cells (data not shown). In contrast, T cells and B cells did not produce IL-6 or MCP-1 upon treatment with vOX2-GST (Fig. 7 and data not shown). These results demonstrate that like cellular OX2, KSHV vOX2 targets myeloid-lineage cells, but unlike cellular OX2, which delivers a negative signal, vOX2 provides an activating signal to myeloid-lineage cells to produce inflammatory cytokines.

Inflammatory cytokine production from U937 monocytes upon incubation with BJAB-vOX2 B lymphocytes. To further examine the effect of vOX2 on monocytes, we analyzed the production of inflammatory cytokines from the U937 monocyte cell line upon incubation with BJAB cells or BJAB-vOX2 cells. IL-1β, TNF-α, and IL-12 production was measured by ELISA after 48 h of incubation of 4×10^5 BJAB or BJAB-vOX2 cells with 1×10^5 U937 cells in the absence or presence of IFN-γ. IFN-γ-stimulated U937 cells produced at least twice the amount of IL-12 and TNF-α upon incubation with BJAB-

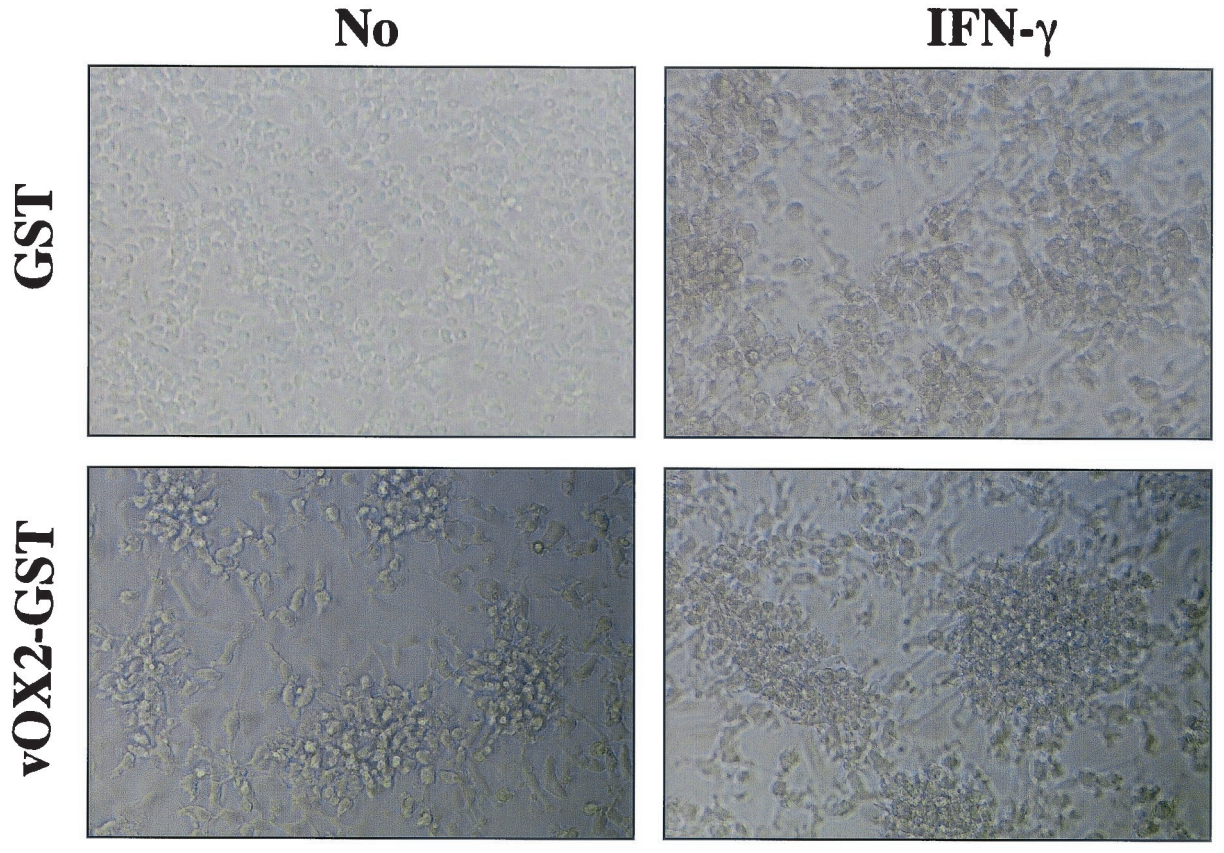

FIG. 6. vOX2-GST protein induces aggregation of dendritic cells. Dendritic cells (10^5) were incubated with 1 μg of GST or vOX2-GST per ml in the absence or presence of IFN-γ (100 U/ml). After 48 h of incubation, cells were photographed with a phase-contrast microscope. Magnification, ×200.

vOX2 cells compared to incubation with BJAB cells (Fig. 8). Unlike primary myeloid cells, mock- and IFN-γ-stimulated U937 cells did not produce detectable IL-1β under any conditions (data not shown). These results demonstrate that surface expression of a full-length vOX2 on B lymphocytes stimulates monocytes to induce inflammatory cytokine production.

DISCUSSION

In this report, we demonstrate that glycosylated KSHV vOX2 protein is expressed on minor populations of unstimulated KSHV infected cells and its expression is further increased during lytic replication. vOX2 protein significantly stimulated primary monocytes, macrophages, and dendritic cells to produce inflammatory cytokines and chemokines, such as IL-1β, IL-6, T 78 F-α, and MCP-1. Furthermore, the surface expression of vOX2 on B lymphocytes stimulated monocyte cells to induce inflammatory cytokine production. These results indicate that like cellular OX2, KSHV vOX2 targets myeloid-lineage cells. However, unlike cellular OX2, which delivers a restrictive signal to myeloid-lineage cells, vOX2 provides an activating signal to myeloid-lineage cells, resulting in the production of inflammatory cytokines.

KS is an inflammatory cytokine-mediated angioproliferative disease, which is triggered by infection of KSHV (12). The lack of chromosomal alterations, the onset of KS as simultaneous multiple lesions in the absence of obvious metastasis, and the sporadic cases of tumor regression further support the role of cytokines in KS development. Furthermore, the nature of the inflammatory infiltrates in KS lesions seems important, since their appearance precedes transformation of the spindle-shaped endothelial cells that harbor KSHV infection (10–12). Immunohistochemistry has shown that these inflammatory infiltrates are prevalently $CD8^+$ T cells, $CD14^+$ and $CD68^+$ monocytes/macrophages, $FXIIIa^+$ dendritic cells, and $CD19^+$ and $CD20^+$ B cells (14, 29, 36, 46). These infiltrates produce a variety of inflammatory cytokines, in particular IFN-γ, IL-1β, and TNF-α, which activate endothelial cells to produce angiogenic factors and act in the recruitment of T cells. Our results suggest that KSHV vOX2 targets and activates infiltrating myeloid-lineage cells to produce inflammatory cytokines, which potentially facilitate the angiogenic proliferation of KS lesions.

KSHV from several PEL lines, including JSC-1 cells, is under tight transcriptional control and remains in a latent state without TPA treatment. KSHV vOX2 is expressed from a 2.7- to 2.8-kb bicistronic transcript in which vOX2 is upstream of the viral G protein-coupled receptor. In agreement with previous reports that vOX2 and the viral G protein-coupled receptor are expressed during early lytic replication (25, 31), we find that vOX2 expression is significantly induced during lytic replication. However, we also observed that a detectable level

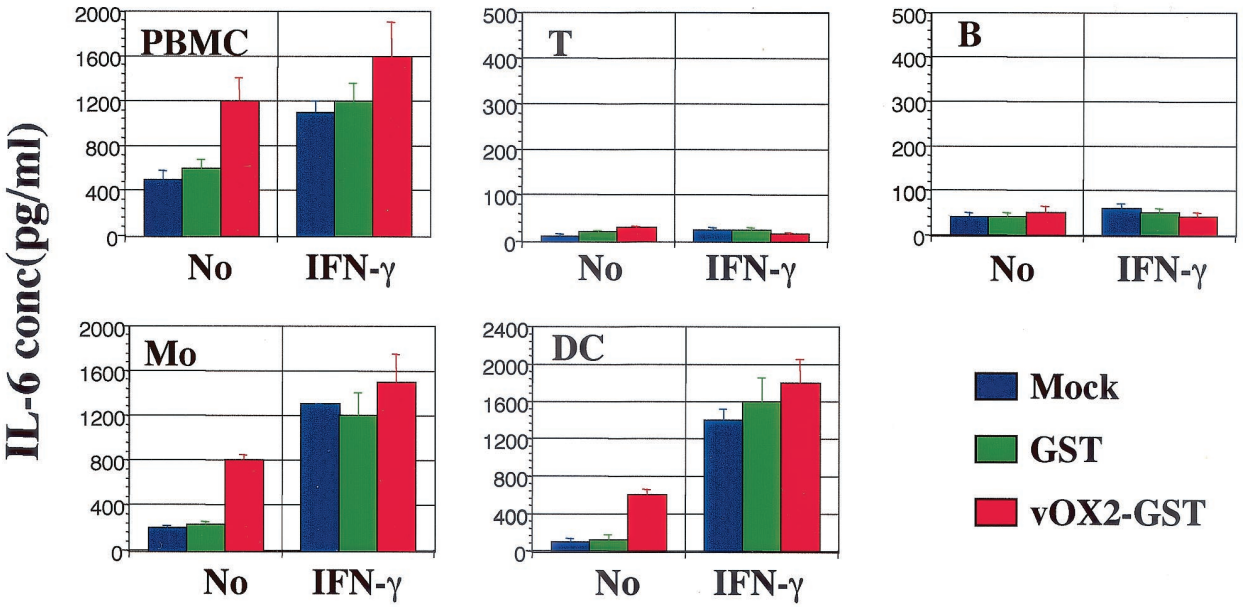

FIG. 7. vOX2-GST protein targets myeloid-lineage cells to induce IL-6 cytokine production. T cells (T), B cells (B), monocytes/macrophages (Mo), and dendritic cells (DC) were sorted by flow cytometry. Each lymphocyte (10^5) was incubated with 1 μg of GST or vOX2-GST per ml or medium as a mock treatment in the absence or presence of IFN-γ (100 U/ml). At 48 h postincubation, the supernatants were harvested and measured for production of IL-6 by ELISA. Data are averages from triplicate measurements, and error bars indicate standard deviations.

of vOX2 protein was expressed on a minor population of unstimulated PEL cells. Recent sensitive DNA arrays have also demonstrated that vOX2 transcript is detectable before TPA stimulation and is increased up to 168-fold by TPA stimulation (22, 37). Thus, it appears that the positive signal of vOX2 during latency is potentially from a minority of spontaneously lytic PELs. However, it is also possible that vOX2 is latently expressed on a minor population of PEL cells, that a minor population of PEL cells expressing vOX2 may undergo abortive lytic replication, or that the stability of vOX2 protein is much higher than that of its mRNA. Further studies should be undertaken to determine a detailed gene expression profile of vOX2 in KSHV-infected PELs and KS lesions.

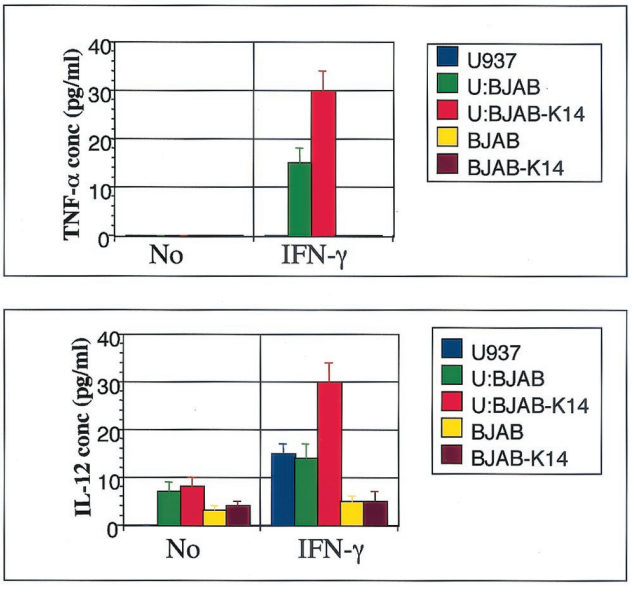

FIG. 8. Inflammatory cytokine production from U937 monocytes upon incubation with BJAB-vOX2 B lymphocytes. U937 cells (1×10^5) were incubated with BJAB cells or BJAB-vOX2 cells (4×10^5) in the absence or presence of IFN-γ (200 U/ml) for 48 h. Unstimulated or IFN-γ-stimulated U937 cells (U), BJAB cells, or BJAB-vOX2 cells were used as controls. The supernatants were harvested and measured for the production of TNF-α and IL-12 by ELISA. Data are averages from triplicate measurements, and error bars indicate standard deviations.

Interestingly, several viruses contain a homologue of cellular OX2. These include KSHV K14 (7), RRV R14 (8, 45), human herpesvirus 6 U85 (16), human herpesvirus 7 U85 (34), Shope fibroma virus S141R (47), myxoma virus M141R (4), Yaba-like disease virus 140R (27), and Yaba monkey tumor virus Yb-C2R (24). Because of the diversity of these viruses, it appears that they might have independently captured the cellular OX2 gene and that the presence of OX2 homology may provide a significant selective advantage to viruses during coevolution with the host. However, we surprisingly find that unlike cellular OX2, KSHV vOX2 provides an activating signal to myeloid-lineage cells to induce inflammatory cytokine production. So, how does vOX2 activate myeloid cells despite sequence similarity with cellular OX2? Conformational alteration of OX2R induced by vOX2 interaction may differ significantly from that induced by cellular OX2 interaction, or vOX2 may interact with receptors on myeloid-lineage cells other than OX2R. Alternatively, vOX2 may neutralize cellular OX2 activity, resulting in the elimination of a restrictive signal and in turn the acquisition of a positive signal. Studies to improve our understanding of the molecular nature of vOX2 function are under way. In summary, we demonstrate a novel viral strategy whereby KSHV has acquired the cellular OX2 gene to activate monocytes, macrophages, and dendritic cells to induce inflam-

matory cytokine production, which potentially promotes the cytokine-mediated angiogenic proliferation of virus-infected cells. In addition, these cytokines may be involved in recruiting lymphocytes to the site of the infection to disseminate virus throughout the infected host. Thus, a detailed study of the molecular mechanisms of myeloid cell activation by KSHV vOX2 not only will lead to a better understanding of viral persistence and disease progression but also will provide a novel means of investigating cellular signal transduction pathways.

ACKNOWLEDGMENTS

We especially thank R. Ambinder for providing JSC-1 cells, N. Barclay for providing OX2 DNA, and M. Connole for flow cytometry analysis.

This work was partly supported by U.S. Public Health Service grants CA82057, CA91819, and RR00168 and ACS grant RPG001102. J. U. Jung is a Leukemia & Lymphoma Society Scholar, and R. E. Means is a Cancer Research Institute Fellow.

REFERENCES

1. **Alexander, L., L. Denekamp, A. Knapp, M. R. Auerbach, B. Damania, and R. C. Desrosiers.** 2000. The primary sequence of rhesus monkey rhadinovirus isolate 26–95: sequence similarities to Kaposi's sarcoma-associated herpesvirus and rhesus monkey rhadinovirus isolate 17577. J. Virol. **74:**3388–3398.
2. **Borriello, F., J. Lederer, S. Scott, and A. H. Sharpe.** 1997. MRC OX-2 defines a novel T cell costimulatory pathway. J. Immunol. **158:**4548–4554.
3. **Browning, P. J., J. M. Sechler, M. Kaplan, R. H. Washington, R. Gendelman, R. Yarchoan, B. Ensoli, and R. C. Gallo.** 1994. Identification and culture of Kaposi's sarcoma-like spindle cells from the peripheral blood of human immunodeficiency virus-1-infected individuals and normal controls. Blood **84:**2711–2720.
4. **Cameron, C., S. Hota-Mitchell, L. Chen, J. Barrett, J. X. Cao, C. Macaulay, D. Willer, D. Evans, and G. McFadden.** 1999. The complete DNA sequence of myxoma virus. Virology **264:**298–318.
5. **Cannon, J. S., D. Ciufo, A. L. Hawkins, C. A. Griffin, M. J. Borowitz, G. S. Hayward, and R. F. Ambinder.** 2000. A new primary effusion lymphoma-derived cell line yields a highly infectious Kaposi's sarcoma herpesvirus-containing supernatant. J. Virol. **74:**10187–10193.
6. **Cesarman, E., Y. Chang, P. S. Moore, J. W. Said, and D. M. Knowles.** 1995. Kaposi's sarcoma-associated herpesvirus-like DNA sequences in AIDS-related body-cavity-based lymphomas. N. Engl. J. Med. **332:**1186–1191.
7. **Chang, Y., E. Cesarman, M. S. Pessin, F. Lee, J. Culpepper, D. M. Knowles, and P. S. Moore.** 1994. Identification of herpesvirus-like DNA sequences in AIDS-associated Kaposi's sarcoma. Science **266:**1865–1869.
8. **Desrosiers, R. C., V. G. Sasseville, S. C. Czajak, X. Zhang, K. G. Mansfield, A. Kaur, R. P. Johnson, A. A. Lackner, and J. U. Jung.** 1997. A herpesvirus of rhesus monkeys related to the human Kaposi's sarcoma-associated herpesvirus. J. Virol. **71:**9764–9769.
9. **Duboise, M., J. Guo, S. Czajak, H. Lee, R. Veazey, R. C. Desrosiers, and J. U. Jung.** 1998. A role for herpesvirus saimiri orf14 in transformation and persistent infection. J. Virol. **72:**6770–6776.
10. **Ensoli, B., C. Sgadari, G. Barillari, M. C. Sirianni, M. Sturzl, and P. Monini.** 2001. Biology of Kaposi's sarcoma. Eur. J. Cancer **37:**1251–1269.
11. **Ensoli, B., and M. Sturzl.** 1998. Kaposi's sarcoma: a result of the interplay among inflammatory cytokines, angiogenic factors and viral agents. Cytokine Growth Factor Rev. **9:**63–83.
12. **Ensoli, B., M. Sturzl, and P. Monini.** 2000. Cytokine-mediated growth promotion of Kaposi's sarcoma and primary effusion lymphoma. Semin. Cancer Biol. **10:**367–381.
13. **Fiorelli, V., R. Gendelman, F. Samaniego, P. D. Markham, and B. Ensoli.** 1995. Cytokines from activated T cells induce normal endothelial cells to acquire the phenotypic and functional features of AIDS-Kaposi's sarcoma spindle cells. J. Clin. Investig. **95:**1723–1734.
14. **Fiorelli, V., R. Gendelman, M. C. Sirianni, H. K. Chang, S. Colombini, P. D. Markham, P. Monini, J. Sonnabend, A. Pintus, R. C. Gallo, and B. Ensoli.** 1998. Gamma-interferon produced by CD8+ T cells infiltrating Kaposi's sarcoma induces spindle cells with angiogenic phenotype and synergy with human immunodeficiency virus-1 Tat protein: an immune response to human herpesvirus-8 infection? Blood **91:**956–967.
15. **Goldman, L. A., E. C. Cutrone, S. V. Kotenko, C. D. Krause, and J. A. Langer.** 1996. Modifications of vectors pEF-BOS, pcDNA1 and pcDNA3 result in improved convenience and expression. BioTechniques **21:**1013–1015.
16. **Gompels, U. A., J. Nicholas, G. Lawrence, M. Jones, B. J. Thomson, M. E. Martin, S. Efstathiou, M. Craxton, and H. A. Macaulay.** 1995. The DNA sequence of human herpesvirus-6: structure, coding content, and genome evolution. Virology **209:**29–51.
17. **Gorczynski, L., Z. Chen, J. Hu, Y. Kai, J. Lei, V. Ramakrishna, and R. M. Gorczynski.** 1999. Evidence that an OX-2-positive cell can inhibit the stimulation of type 1 cytokine production by bone marrow-derived B7–1 (and B7–2)-positive dendritic cells. J. Immunol. **162:**774–781.
18. **Gorczynski, R. M., M. S. Cattral, Z. Chen, J. Hu, J. Lei, W. P. Min, G. Yu, and J. Ni.** 1999. An immunoadhesin incorporating the molecule OX-2 is a potent immunosuppressant that prolongs allo- and xenograft survival. J. Immunol. **163:**1654–1660.
19. **Gorczynski, R. M., Z. Chen, X. M. Fu, and H. Zeng.** 1998. Increased expression of the novel molecule OX-2 is involved in prolongation of murine renal allograft survival. Transplantation **65:**1106–1114.
20. **Hoek, R. M., S. R. Ruuls, C. A. Murphy, G. J. Wright, R. Goddard, S. M. Zurawski, B. Blom, M. E. Homola, W. J. Streit, M. H. Brown, A. N. Barclay, and J. D. Sedgwick.** 2000. Down-regulation of the macrophage lineage through interaction with OX2 (CD200). Science **290:**1768–1771.
21. **Ishido, S., C. Wang, B. S. Lee, G. B. Cohen, and J. U. Jung.** 2000. Down-regulation of major histocompatibility complex class I molecules by Kaposi's sarcoma-associated herpesvirus K3 and K5 proteins. J. Virol. **74:**5300–5309.
22. **Jenner, R. G., M. M. Alba, C. Boshoff, and P. Kellam.** 2001. Kaposi's sarcoma-associated herpesvirus latent and lytic gene expression as revealed by DNA arrays. J. Virol. **75:**891–902.
23. **Kedes, D. H., M. Lagunoff, R. Renne, and D. Ganem.** 1997. Identification of the gene encoding the major latency-associated nuclear antigen of the Kaposi's sarcoma-associated herpesvirus. J. Clin. Investig. **100:**2606–2610.
24. **Kilpatrick, D. R., and H. Rouhandeh.** 1985. Cloning and physical mapping of Yaba monkey tumor virus DNA. Virology **143:**399–406.
25. **Kirshner, J. R., K. Staskus, A. Haase, M. Lagunoff, and D. Ganem.** 1999. Expression of the open reading frame 74 (G-protein-coupled receptor) gene of Kaposi's sarcoma (KS)-associated herpesvirus: implications for KS pathogenesis. J. Virol. **73:**6006–6014.
26. **Kraffert, C., L. Planus, and N. S. Penneys.** 1991. Kaposi's sarcoma: further immunohistologic evidence of a vascular endothelial origin. Arch. Dermatol. **127:**1734–1735.
27. **Lee, H. J., K. Essani, and G. L. Smith.** 2001. The genome sequence of Yaba-like disease virus, a yatapoxvirus. Virology **281:**170–192.
28. **Li, M., J. MacKey, S. C. Czajak, R. C. Desrosiers, A. A. Lackner, and J. U. Jung.** 1999. Identification and characterization of Kaposi's sarcoma-associated herpesvirus K8.1 virion glycoprotein. J. Virol. **73:**1341–1349.
29. **MacPhail, L. A., N. P. Dekker, and J. A. Regezi.** 1996. Macrophages and vascular adhesion molecules in oral Kaposi's sarcoma. J. Cutan. Pathol. **23:**464–472.
30. **Mesri, E. A., E. Cesarman, L. Arvanitakis, S. Rafii, M. A. Moore, D. N. Posnett, D. M. Knowles, and A. S. Asch.** 1996. Human herpesvirus-8/Kaposi's sarcoma-associated herpesvirus is a new transmissible virus that infects B cells. J. Exp. Med. **183:**2385–2390.
31. **Nador, R. G., L. L. Milligan, O. Flore, X. Wang, L. Arvanitakis, D. M. Knowles, and E. Cesarman.** 2001. Expression of Kaposi's sarcoma-associated herpesvirus G protein-coupled receptor monocistronic and bicistronic transcripts in primary effusion lymphomas. Virology **287:**62–70.
32. **Neipel, F., J. C. Albrecht, and B. Fleckenstein.** 1997. Cell-homologous genes in the Kaposi's sarcoma-associated rhadinovirus human herpesvirus 8: determinants of its pathogenicity? J. Virol. **71:**4187–4192.
33. **Neipel, F., and B. Fleckenstein.** 1999. The role of HHV-8 in Kaposi's sarcoma. Semin. Cancer Biol. **9:**151–164.
34. **Nicholas, J.** 1996. Determination and analysis of the complete nucleotide sequence of human herpesvirus. J. Virol. **70:**5975–5989.
35. **Nicholas, J., V. Ruvolo, J. Zong, D. Ciufo, H. G. Guo, M. S. Reitz, and G. S. Hayward.** 1997. A single 13-kilobase divergent locus in the Kaposi sarcoma-associated herpesvirus (human herpesvirus 8) genome contains nine open reading frames that are homologous to or related to cellular proteins. J. Virol. **71:**1963–1974.
36. **Nickoloff, B. J., and C. E. Griffiths.** 1989. Factor XIIIa-expressing dermal dendrocytes in AIDS-associated cutaneous Kaposi's sarcomas. Science **243:**1736–1737.
37. **Paulose-Murphy, M., N. K. Ha, C. Xiang, Y. Chen, L. Gillim, R. Yarchoan, P. Meltzer, M. Bittner, J. Trent, and S. Zeichner.** 2001. Transcription program of human herpesvirus 8 (Kaposi's sarcoma-associated herpesvirus). J. Virol. **75:**4843–4853.
38. **Rainbow, L., G. M. Platt, G. R. Simpson, R. Sarid, S. J. Gao, H. Stoiber, C. S. Herrington, P. S. Moore, and T. F. Schulz.** 1997. The 222- to 234-kilodalton latent nuclear protein (LNA) of Kaposi's sarcoma-associated herpesvirus (human herpesvirus 8) is encoded by orf73 and is a component of the latency-associated nuclear antigen. J. Virol. **71:**5915–5921.
39. **Regezi, J. A., L. A. MacPhail, T. E. Daniels, Y. G. DeSouza, J. S. Greenspan, and D. Greenspan.** 1993. Human immunodeficiency virus-associated oral Kaposi's sarcoma. A heterogeneous cell population dominated by spindle-shaped endothelial cells. Am. J. Pathol. **143:**240–249.
40. **Reitz, M. S., Jr., L. S. Nerurkar, and R. C. Gallo.** 1999. Perspective on Kaposi's sarcoma: facts, concepts, and conjectures. J. Natl. Cancer Inst. **91:**1453–1458.

41. **Renne, R., M. Lagunoff, W. Zhong, and D. Ganem.** 1996. The size and conformation of Kaposi's sarcoma-associated herpesvirus (human herpesvirus 8) DNA in infected cells and virions. J. Virol. **70:**8151–8154.
42. **Russo, J. J., R. A. Bohenzky, M. C. Chien, J. Chen, M. Yan, D. Maddalena, J. P. Parry, D. Peruzzi, I. S. Edelman, Y. Chang, and P. S. Moore.** 1996. Nucleotide sequence of the Kaposi sarcoma-associated herpesvirus (HHV8). Proc. Natl. Acad. Sci. USA **93:**14862–14867.
43. **Ruszczak, Z., A. Mayer-Da Silva, and C. E. Orfanos.** 1987. Kaposi's sarcoma in AIDS. Multicentric angioneoplasia in early skin lesions. Am. J. Dermatopathol. **9:**388–398.
44. **Sarid, R., O. Flore, R. A. Bohenzky, Y. Chang, and P. S. Moore.** 1998. Transcription mapping of the Kaposi's sarcoma-associated herpesvirus (human herpesvirus 8) genome in a body cavity-based lymphoma cell line (BC-1). J. Virol. **72:**1005–1012.
45. **Searles, R. P., E. P. Bergquam, M. K. Axthelm, and S. W. Wong.** 1999. Sequence and genomic analysis of a rhesus macaque rhadinovirus with similarity to Kaposi's sarcoma-associated herpesvirus/human herpesvirus 8. J. Virol. **73:**3040–3053.
46. **Uccini, S., L. P. Ruco, F. Monardo, A. Stoppacciaro, E. Dejana, I. L. La Parola, D. Cerimele, and C. D. Baroni.** 1994. Co-expression of endothelial cell and macrophage antigens in Kaposi's sarcoma cells. J. Pathol. **173:**23–31.
47. **Willer, D. O., G. McFadden, and D. H. Evans.** 1999. The complete genome sequence of Shope (rabbit) fibroma virus. Virology **264:**319–343.
48. **Wright, G. J., M. J. Puklavec, A. C. Willis, R. M. Hoek, J. D. Sedgwick, M. H. Brown, and A. N. Barclay.** 2000. Lymphoid/neuronal cell surface OX2 glycoprotein recognizes a novel receptor on macrophages implicated in the control of their function. Immunity **13:**233–242.